International Journal of Nanomedicine

Dovepress
open access to scientific and medical research

Open Access Full Text Article

ORIGINAL RESEARCH

Nanogel-crosslinked nanoparticles increase the inhibitory effects of W9 synthetic peptide on bone loss in a murine bone resorption model

This article was published in the following Dove Press journal:
International Journal of Nanomedicine
11 May 2015
Number of times this article has been viewed

Toshimi Sato[1]
Neil Alles[1,2]
Masud Khan[1,3]
Kenichi Nagano[1,4]
Mariko Takahashi[1]
Yukihiko Tamura[1]
Asako Shimoda[5,6]
Keiichi Ohya[1]
Kazunari Akiyoshi[5,6]
Kazuhiro Aoki[1]

[1]Department of Bio-Matrix (Pharmacology), Graduate School, Tokyo Medical and Dental University, Tokyo, Japan; [2]Department of Biochemistry, Faculty of Medicine, University of Peradeniya, Peradeniya, Sri Lanka; [3]Department of Dental Pharmacology, City Dental College and Hospital, Dhaka, Bangladesh; [4]Department of Oral Medicine, Infection and Immunity, Harvard School of Dental Medicine, Boston, MA, USA; [5]Department of Polymer Chemistry, Graduate School of Engineering, Kyoto University, Katsura, [6]ERATO Akiyoshi Bio-Nanotransporter Project, Japan Science and Technology Agency, Katsura Int'tech Center Kyotodaigaku-Katsura, Nishikyo-ku, Kyoto, Japan

Correspondence: Kazuhiro Aoki
Department of Bio-Matrix (Pharmacology), Graduate School, Tokyo Medical and Dental University, 1-5-45 Yushima, Bunkyo-ku, Tokyo 113-8549, Japan
Tel +81 3 5803 5461
Fax +81 3 5803 0190
Email kazu.hpha@tmd.ac.jp

Abstract: We investigated the biological activity of W9, a bone resorption inhibitor peptide, using NanoClik nanoparticles as an injectable carrier, where acryloyl group-modified cholesterol-bearing pullulan (CHPOA) nanogels were crosslinked by pentaerythritol tetra (mercaptoethyl) polyoxyethylene. Thirty 5-week-old male C57BL/6J mice were fed a low calcium diet and received once-daily subcutaneous injections of the carrier alone, W9 24 mg/kg/day alone, W9 24 mg/kg/day incorporated in cholesterol bearing pullulan (CHP) nanogels, or W9 (8 and 24 mg/kg/day) incorporated in NanoClik nanoparticles for 4 days (n=5). Mice that received a normal calcium diet with NanoClik nanoparticle injections without W9 were used as a control group. Radiological analyses showed that administration of W9 24 mg/kg/day significantly prevented low calcium-induced reduction of bone mineral density in the long bones and lumbar vertebrae, but only when the NanoClik nanoparticles were used as a carrier. Histomorphometric analyses of the proximal tibiae revealed that W9 24 mg/kg/day incorporated in NanoClik nanoparticles prevented the increase in bone resorption indices induced by a low calcium diet, which was confirmed by measurement of serum bone resorption markers. These data suggest that NanoClik nanoparticles could be a useful carrier for peptide therapeutics, and also demonstrate that daily subcutaneous injections of the W9 peptide with the nanoparticles were able to inhibit bone loss in vivo. An osteoclastogenesis inhibition assay performed in vitro confirmed a slower release profile of W9 from NanoClik nanoparticles compared with conventional CHP nanogels.

Keywords: nanocarrier, peptide drug, injectable drug carrier, polyethylene glycol crosslinking, cholesterol-bearing pullulan, controlled release

Introduction

Peptides have attracted a great deal of attention as therapeutic molecules for novel drug discovery, since they can be modified to fit specific drug targets. Peptides are also able to be fully synthesized, thereby allowing them to be produced at a lower cost than macromolecular drugs, such as antibodies.[1–3] However, approximately 95% of peptide drug candidates do not reach clinical application, largely because peptides have a short biological half-life as a result of their low stability in the systemic circulation and/or autoaggregation.[4] Therefore, an appropriate drug delivery system to overcome these problems is required for development of therapeutic peptides.

Various protein and peptide delivery systems using nanocarriers have been reported to show sustained release.[5–10] Among these drug delivery systems, cholesterol-bearing pullulan (CHP), which is composed of nanometer-sized polymer hydrogel particles (nanogels), has been shown to be a suitable delivery system for proteins.[11–14] While preventing the aggregation of proteins, CHP nanogels can also trap various proteins

inside through hydrophobic interactions, and can release them in their native form by exchanging them with other surrounding proteins, such as serum albumin.[11] CHP nanogels have been shown to be a safe carrier, since they have been tested in clinical studies as a carrier for cancer therapeutics.[15,16] However, CHP nanogels rapidly release the proteins incorporated in the complex in the bloodstream following displacement of the protein by serum proteins,[17] presumably because CHP nanogels are crosslinked exclusively by physical forces, without any covalent interactions.[17,18]

Modification of molecules by polyethylene glycol (PEG) is often performed to enhance drug retention,[19–21] and this PEGylation has been proven to induce favorable pharmacokinetics and to reduce the toxicity and immunogenicity of drugs.[22] Injectable nanocarriers (NanoClik nanoparticles)[10] where the acryloyl group has been modified in cholesterol-bearing pullulan (CHPOA) nanogels crosslinked by pentaerythritol tetra (mercaptoethyl) polyoxyethylene (PEGSH) have been synthesized to overcome the rapid release of the incorporated protein from the CHP nanogels.[18,23] Transmission electron microscopy images of NanoClik nanoparticles showed that the nanogels were gathered together to form one particle, which was a raspberry-like structure.[18] The chemical crosslinking of nanogels with PEG derivatives has allowed for prevention of non-specific protein adsorption,[18,24,25] thereby slowing the exchange rate of an incorporated protein with serum proteins. Furthermore, the NanoClik nanoparticles also provide higher structural stability when compared with conventional CHP nanogels.[18]

The W9 peptide is an inhibitor of osteoclast formation that acts by antagonizing the effects of the receptor activator of nuclear factor kappa B ligand (RANKL), a critical molecule required for osteoclastogenesis.[26,27] W9 efficiently prevented bone loss by inhibiting osteoclast formation in murine bone resorption models in vivo, including a low calcium diet model.[26,28–30] However, eight daily subcutaneous injections (every 3 hours) or a subcutaneously implanted osmotic pump were required for this peptide to achieve efficient prevention of bone loss in these models.[26,28,31,32] Despite its activity, few studies have so far been performed to find a suitable carrier for the peptide drug candidate W9 with an eye towards clinical application of the molecule.

Nanocarriers (nanohydroxyapatite/collagen/porous polylactic acid) were reportedly used for another peptide therapeutic, P-24, a mimic of bone morphogenetic protein,[10] but the release profile of the peptide has not been examined, even in in vitro studies.

In the present study, we report the use of NanoClik nanoparticles as an injectable carrier for a peptide drug, and demonstrate the inhibitory effects of once-daily W9 injection via these nanoparticles on osteoclast formation and bone loss in a murine bone resorption model. The release profile of W9 from NanoClik nanoparticles was also investigated using an osteoclastogenesis inhibition assay.

Materials and methods

Animals

Thirty 5-week-old male C57BL/6J mice were purchased from CLEA Japan (Tokyo, Japan). The mice were maintained under a 12-hour light/dark cycle in our animal care facilities,[26] and the experimental procedures were reviewed and approved by the Institutional Animal Care and Use Committee of Tokyo Medical and Dental University (authorizations 100182, 0120217A, and 0150203A).

Materials

W9 was purchased from the American Peptide Company (Sunnyvale, CA, USA). CHP nanogels and CHPOA nanogels were synthesized as described elsewhere.[18] PEGSH (molecular weight 1.0×10^4 g/mol) was purchased from NOF Co (Tokyo, Japan).[18] Nuclear magnetic resonance characterization of the CHPOA nanogels and NanoClik nanoparticles has been described previously.[18] CHPOA nanogels were suspended in phosphate-buffered saline at 10 mg/mL. The suspension was mixed with a solution of W9 and kept overnight at 4°C to form the CHPOA-W9 complex. When we tried to incorporate 6 mg W9 in the 30 mg/mL nanogel, it was difficult to form a gel-type structure. Therefore, we assumed that the maximum dose of W9 able to be incorporated was 20% of the concentration of the CHP nanogel.[29] Since we used 5.0 mg/mL CHP nanogels in this study, 1 mg of W9 peptide per mL was the maximum.

The CHPOA-W9 complex was mixed with PEGSH (9.4 mg/mL) at a molar ratio of 4:1 for the acryloyl groups on the CHPOA nanogels, and the mixture was incubated for 24 hours at 37°C under a humidified atmosphere (the final concentration of CHPOA nanogels was 5 mg/mL). NanoClik nanoparticles were formed as shown in Figure 1. In the same way, the CHPOA-W9 complex was crosslinked with PEGSH by Michael addition to generate the W9 incorporated in the NanoClik nanoparticles, and was kept at 4°C until use.

Measurement of hydrodynamic diameters

The hydrodynamic diameters of W9, W9 incorporated in CHP nanogels, W9 incorporated in CHPOA nanogels, and

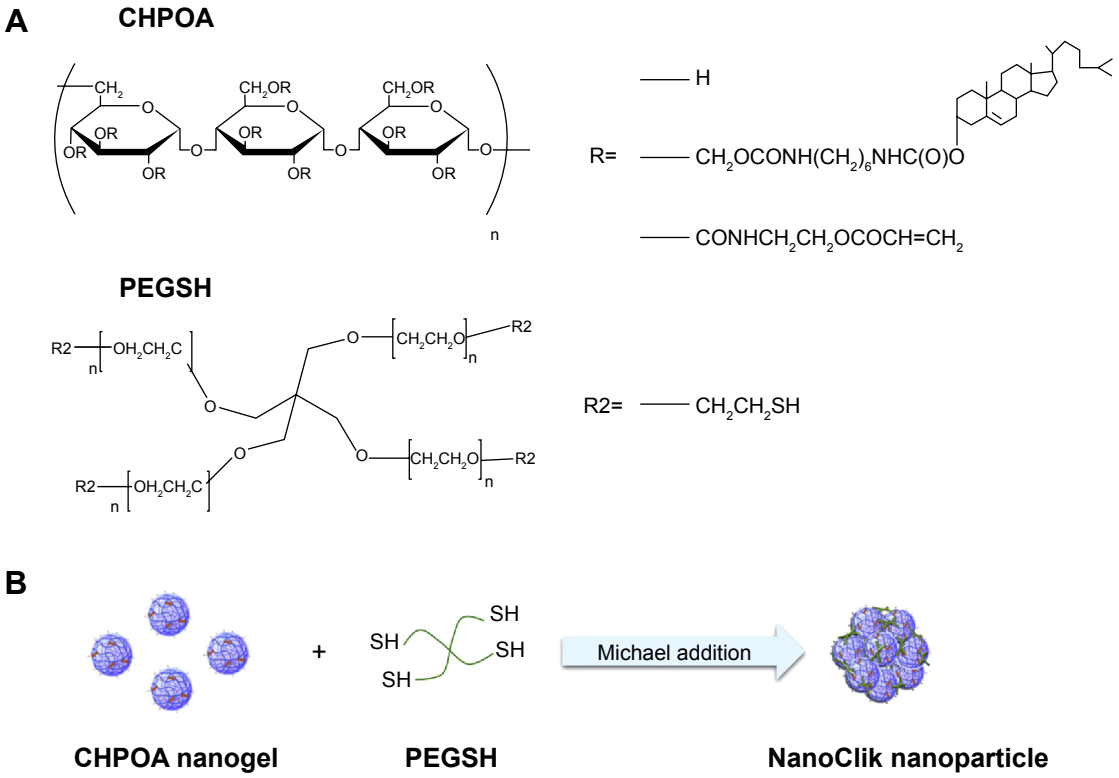

Figure 1 Schematic illustration of NanoClik nanoparticle formation. (**A**) Chemical structures of the CHPOA and PEGSH. (**B**) CHPOA were crosslinked with PEGSH by Michael addition.
Abbreviations: CHPOA, acryloyl group-modified cholesterol-bearing pullulan; PEGSH, pentaerythritol tetra (mercaptoethyl) polyoxyethylene.

W9 incorporated in PEGSH-crosslinked CHPOA nanogels (NanoClik nanoparticles) were evaluated by dynamic light scattering (Zetasizer Nano series, Malvern Instruments, Malvern, UK) as described previously.[18]

Experimental protocol using a bone resorption model induced by a low calcium diet

All mice were housed singly in metabolic cages (Metabolica, Sugiyama-Gen, Tokyo, Japan) and were fed a semi-synthetic diet using a pair feeding technique as described previously.[26,28,30,33] Briefly, all mice were fed a normal calcium diet containing 0.5% calcium and 0.35% phosphorus for 3 days; five mice were then fed a normal calcium diet while the others were fed a low calcium diet containing 0.05% calcium and 0.35% phosphorus for 4 days.

The mice were divided into six groups (n=5 per group) as follows: mice fed a normal calcium diet received a daily injection of NanoClik nanoparticles (abbreviated as normal Ca + NanoClik). The other mice were fed a low calcium diet and received a daily injection of NanoClik nanoparticles as a vehicle control (low Ca + NanoClik), W9 24 mg/kg/day alone (low Ca + W9 24 mg), W9 24 mg/kg/day incorporated in CHP nanogels (low Ca + CHP-W9 24 mg), W9 8 mg/kg/day incorporated in NanoClik nanoparticles (low Ca + NanoClik-W9 8 mg), or W9 24 mg/kg/day incorporated in NanoClik nanoparticles (low Ca + NanoClik-W9 24 mg). Figure 2 shows the group name abbreviations and experimental protocol used in this study. All injections were performed subcutaneously once a day. The mice were sacrificed 4 days after starting the low calcium diet by gentle cervical dislocation under deep sedation with medetomidine hydrochloride (6.6 mg/kg, Domitor®, Zenoaq, Fukushima, Japan).

Radiological assessment of tibiae, femurs, and lumbar vertebrae

The tibiae, femurs, and lumbar vertebrae were dissected, and soft tissues were roughly removed. All of the bones were then fixed in glutaraldehyde 0.5%/formalin 3.7% fixative (pH 7.4) for 3 days at 4°C, and then washed with phosphate-buffered saline for radiological and histological analyses. Three-dimensional reconstruction images of the tibiae, femurs, and lumbar vertebrae were obtained with an image analysis software program (TRI/3D-View, Ratoc

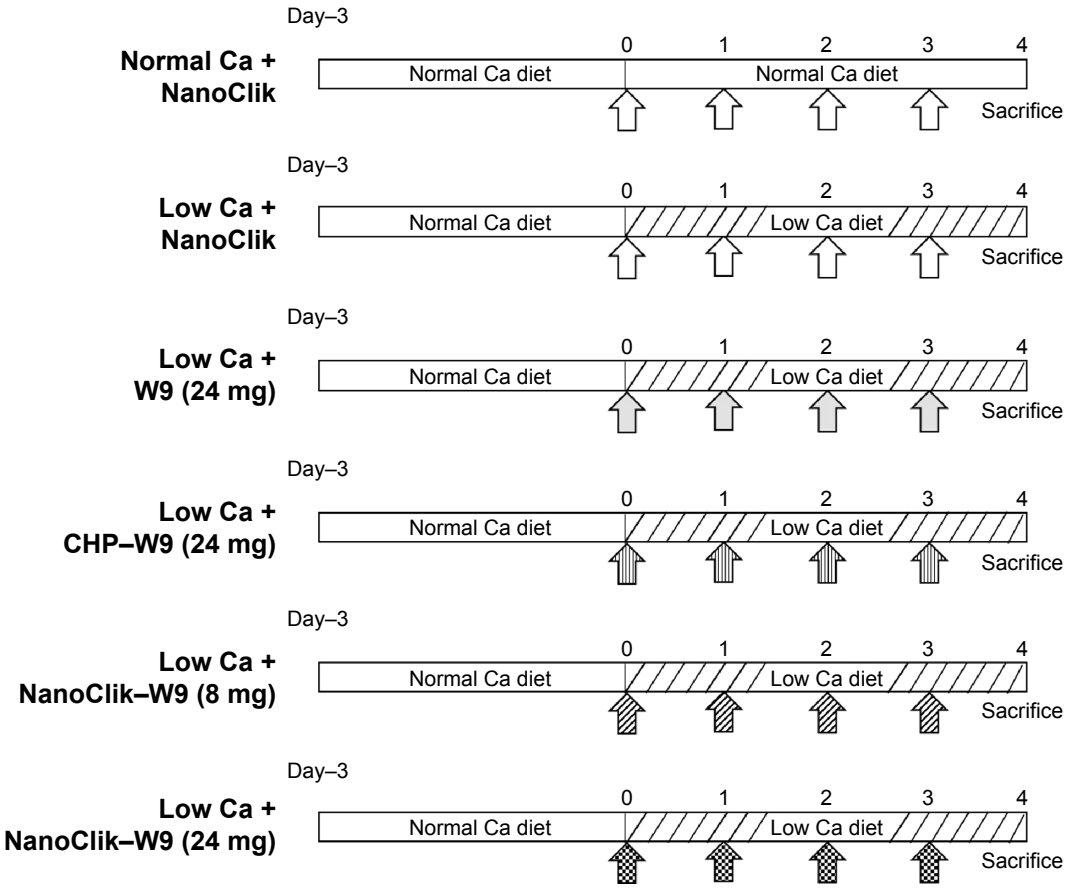

Figure 2 Schematic diagram of experimental protocol for murine bone resorption model induced by a low calcium diet.
Notes: All mice were fed a normal calcium diet containing 0.5% calcium and 0.35% phosphorus for 3 days, and then one group (n=5 per group) was fed a normal calcium diet, while the other five groups were fed a low calcium diet containing 0.05% calcium and 0.35% phosphorus for the next 4 days. The arrows indicate the time points of once-daily subcutaneous injections of vehicle (NanoClik nanoparticles, NanoClik), W9 (24 mg/kg/day) only, W9 (24 mg/kg/day) incorporated in CHP nanogels or W9 (8 and 24 mg/kg/day) incorporated in NanoClik nanoparticles. All mice were sacrificed on day 4 after starting the low calcium diet.
Abbreviations: Ca, calcium; CHP, cholesterol-bearing pullulan.

System Engineering, Tokyo, Japan) using the data obtained by microfocal computed tomography (μ-CT; ScanXmate-E090 [94 mA, 85 mV], Comscan, Kanagawa, Japan). The bone mineral density (BMD) of the tibiae, femurs, and vertebrae (third lumbar) were measured by peripheral quantitative computed tomography (pQCT; XCT Research SA+; Collimation B, Stratec Medizintechnik GmbH, Pforzheim, Germany). The trabecular BMD of the tibiae was analyzed at the proximal metaphysis, the trabecular BMD of the femurs was analyzed at the distal metaphysis, and the trabecular BMD of the lumbar vertebrae was analyzed at the body of the third lumbar vertebrae.[26,28,34]

Histological preparation and bone histomorphometry

For the histological assessments, tibiae were embedded in methyl methacrylate as described previously.[35] Undecalcified sections (5 μm) were prepared using an automicrotome (Supercut 2050, Reichert-Jung, Armsberg, Germany). Some sections were stained with von Kossa stain and counterstained with a modified van Gieson method to clarify the mineralized tissue,[36,37] or were subjected to tartrate-resistant acid phosphatase (TRAP) staining. Osteoclasts were designated as TRAP-positive multinucleated cells (n>2) located on the bone surface. A standard bone histomorphometric analysis[38,39] was performed in the secondary spongiosa of the tibiae using an image analysis system (KS400, Carl Zeiss, Jena, Germany) as described elsewhere.[26,28,37]

Serum biochemical assays

Under deep sedation with medetomidine hydrochloride (Domitor 6.6 mg/kg), blood samples were collected from the orbital sinus of each mouse by puncture just before sacrifice. The serum level of C-terminal telopeptide (CTX), a degradation product of type I collagen, was measured individually in duplicate samples using an enzyme immunoassay

kit (RatLaps EIA, IDS Ltd, Boldon, UK) according to the manufacturer's instructions.[30]

Osteoclastogenesis inhibition assay to clarify W9 release from nanogel carriers and determination of amount of W9 released from NanoClik nanoparticles in vitro

The amount of W9 released from each of the carriers was predicted using an osteoclastogenesis assay modified from the established method.[40,41] First, we cultured bone marrow cells with 25 ng/mL macrophage colony-stimulating factor (R&D Systems, Minneapolis, MN, USA) and 5 ng/mL RANKL (Wako, Osaka, Japan) in the wells of a 48-well plate (Sumitomo Bakelite, Tokyo, Japan) for one day in the presence of 10% fetal bovine serum (Invitrogen, Grand Island, NY, USA) to obtain bone marrow-derived osteoclast precursors using alpha minimal essential medium (Sigma-Aldrich, St Louis, MO, USA) with 100 units of penicillin and 100 μg/mL streptomycin (Sigma-Aldrich). Next, W9 (50 μM), vehicle (0.05% dimethyl sulfoxide), CHP nanogels (CHP), W9 (50 μM incorporated in CHP nanogels [CHP-W9]), NanoClik nanoparticles (NanoClik), and W9 (50 μM incorporated in NanoClik nanoparticles [NanoClik-W9]) were added in the cultures, which were further incubated with 25 ng/mL macrophage colony-stimulating factor and 100 ng/mL RANKL for 3 days in the presence of 10% fetal bovine serum.

Another set of cultures was performed in the same way as described in the previous paragraph using the NanoClik nanoparticles and NanoClik-W9 (50 μM incorporated in NanoClik nanoparticles) in the presence of 50% fetal bovine serum. The cells were fixed using 3.7% phosphate-buffered formalin, and were stained for TRAP. TRAP-positive multinucleated cells (nucleus number >3) were counted. The amount of W9 released from the nanogels was determined from the regression analysis on the graph of TRAP-positive multinucleated cells versus the corresponding W9 concentrations (1, 3, 5, 10, 30, 50, and 100 μM).

Statistical analysis

The data were analyzed by one-way analysis of variance, and when a significant F ratio was identified, groups were compared using Fisher's protected least significant difference post hoc test. The difference was considered to be significant for values with $P<0.05$. All data are presented as the mean ± standard deviation.

Results

Prevention of aggregation of W9 by nanogels

As described in the introduction section, peptide drugs frequently form aggregates, and this aggregation is considered to be one of the reasons why peptides are not able to elicit therapeutic effects. Therefore, an appropriate carrier that can prevent aggregation is necessary to allow the peptide drugs to elicit biological effects. We used W9, a peptide known to inhibit bone resorption, as a representative peptide drug to investigate the feasibility of using NanoClik nanoparticles as a peptide carrier in vivo. First, we measured the hydrodynamic diameters of various complexes to determine whether nanogels could prevent aggregation of the peptide. When the W9 peptide was dispersed at a concentration of 120 mg/mL in phosphate-buffered saline (pH 7.4), large aggregates were observed by dynamic light scattering (the size of the aggregates was 6,054±1,558 nm, polydispersity index 0.34). Once W9 was incorporated in CHP nanogels or CHPOA nanogels, the hydrodynamic diameters were significantly reduced: CHP nanogel, 344±52 nm (polydispersity index 0.53); CHPOA nanogel, 64.4±4.0 nm (polydispersity index 0.50). After crosslinking of the CHPOA-W9 nanogel with PEGSH, the hydrodynamic diameter of the NanoClik nanoparticles was 254±17.6 nm (polydispersity index 0.76).

Effects of NanoClik nanoparticles as a peptide carrier in bone resorption model

As we described in the introduction section, eight daily subcutaneous injections of W9 were found to be required to prevent the bone loss induced by a low calcium diet in mice.[26] In the present study, we examined whether once-daily subcutaneous injections of W9 incorporated in NanoClik nanoparticles could prevent the bone loss induced by a low calcium diet. Three-dimensional reconstruction images of the proximal tibiae from μ-CT scanning data showed that there was trabecular bone loss at the tibial metaphysis in the vehicle-injected low calcium group compared with the vehicle-injected normal calcium group (Figure 3A). As described in the materials and methods section, NanoClik nanoparticles were used as a vehicle for the in vivo study. The higher dose of W9 (24 mg/kg/day) incorporated in NanoClik nanoparticles prevented this decrease of bone, but the lower dose of W9 (8 mg/kg/day) incorporated in NanoClik nanoparticles did not significantly prevent the bone loss induced by a low calcium diet, nor did W9 24 mg/kg/day alone or W9 24 mg/kg/day

incorporated in CHP nanogels (Figure 3A). These μ-CT observations were confirmed by BMD measurements at the tibiae (Figure 3B), femurs (Figure S1), and lumbar vertebrae (Figure S2) by pQCT.

Bone structural parameters of cancellous region at the tibial metaphysis

Nondecalcified sagittal sections of proximal tibiae stained by the von Kossa method showed changes in the amount of mineralized bone in the cancellous region (Figure 4A). Standard bone histomorphometric analyses confirmed the presence of structural changes in the cancellous bone of the tibiae. Structural parameters, including trabecular bone volume and trabecular number, were significantly reduced in the vehicle-injected low calcium group. Once-daily subcutaneous injections of W9 24 mg/kg/day incorporated in NanoClik nanoparticles significantly prevented the low calcium-induced decrease in trabecular bone volume and trabecular number (Figure 4B and C). The other bone structural parameter, trabecular separation, was significantly increased in the vehicle-injected low calcium group compared with the vehicle-injected normal calcium group. Once-daily injections of W9 24 mg/kg/day incorporated in NanoClik nanoparticles significantly prevented the increase in trabecular separation induced by a low calcium diet (Figure 4D). However, no significant changes in trabecular thickness were observed in the other groups (Figure 4E).

Once-daily injections of W9 incorporated in NanoClik nanoparticles prevented bone resorption induced by a low calcium diet

Histological sections of the proximal tibiae showed that TRAP-positive cells in the vehicle-injected low calcium group seemed to be increased compared with those in the vehicle-injected normal calcium group. Treatment with W9 24 mg/kg/day incorporated in NanoClik nanoparticles

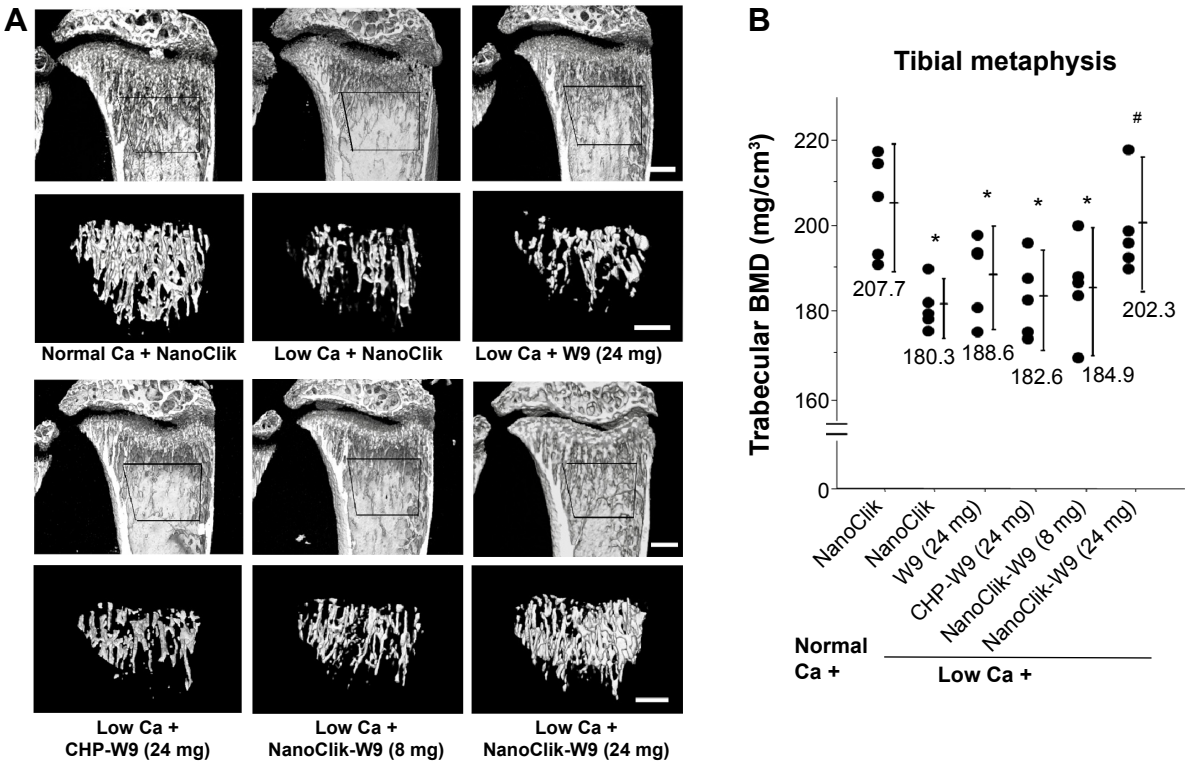

Figure 3 Findings of radiological assessments of the proximal tibiae.

Notes: (**A**) Three-dimensional reconstruction microfocal CT images of the proximal tibiae (upper panel) and the secondary spongiosa in the metaphysis of the proximal tibiae (lower panel). The trapezoidal frame in the upper panels indicates the area shown in the magnified images in the lower panels. The scale bar represents 500 μm. (**B**) Trabecular BMD of the proximal tibiae measured by peripheral quantitative CT. The six experimental groups shown in the figure are as follows: normal Ca + NanoClik (n=5), vehicle (NanoClik nanoparticle)-injected mice fed a normal calcium diet; low Ca + NanoClik (n=5), vehicle (NanoClik nanoparticle)-injected mice fed a low calcium diet; low Ca + W9 (24 mg, n=5), W9 (24 mg/kg/day) was injected into mice fed a low calcium diet; low Ca + CHP-W9 (24 mg, n=5), W9 (24 mg/kg/day) incorporated in CHP nanogels was injected into mice fed a low calcium diet; low Ca + NanoClik-W9 (8 mg, n=5), W9 (8 mg/kg/day) incorporated in NanoClik nanoparticles was injected into mice fed a low calcium diet; low Ca + NanoClik-W9 (24 mg, n=5), W9 (24 mg/kg/day) incorporated in NanoClik nanoparticles was injected into mice fed a low calcium diet. Data are shown as the mean ± standard deviation, with n=5 for each experimental group. $^{*}P<0.05$ versus normal Ca + NanoClik; $^{\#}P<0.05$ versus low Ca + NanoClik.

Abbreviations: BMD, bone mineral density; Ca, calcium; CHP, cholesterol-bearing pullulan; CT, computed tomography.

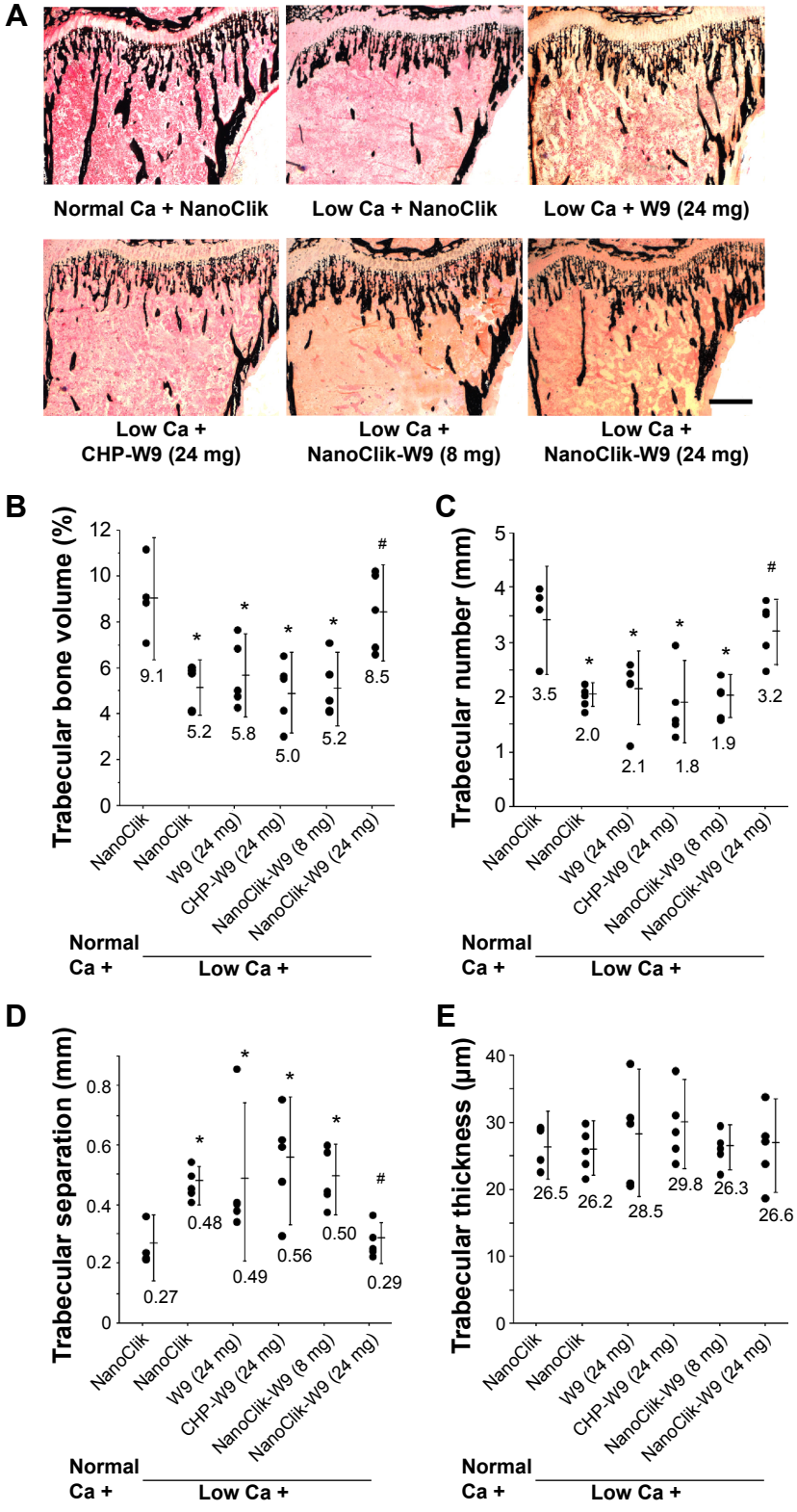

Figure 4 Mineralized tissue in cancellous region of tibial metaphysis.

Notes: (**A**) Photomicrographs of undecalcified sagittal sections (5 μM) of the proximal tibiae with von Kossa staining and counterstained using a modified van Gieson method. The scale bar represents 500 μm. The area of mineralized tissue is shown in black. (**B**) Trabecular bone volume, (**C**) trabecular number, (**D**) trabecular separation, and (**E**) trabecular thickness. Data are shown as the mean ± standard deviation, with n=5 for each experimental group. $^{*}P<0.05$ versus normal Ca + NanoClik; $^{\#}P<0.05$, versus low Ca + NanoClik.

Abbreviations: BMD, bone mineral density; Ca, calcium; CHP, cholesterol-bearing pullulan; Normal Ca + NanoClik (n=5), vehicle (NanoClik nanoparticle)-injected mice fed a normal calcium diet; low Ca + NanoClik (n=5), vehicle (NanoClik nanoparticle)-injected mice fed a low calcium diet; low Ca + W9 (24 mg, n=5), W9 (24 mg/kg/day) was injected into mice fed a low calcium diet; low Ca + CHP-W9 (24 mg, n=5), W9 (24 mg/kg/day) incorporated in CHP nanogels was injected into mice fed a low calcium diet; low Ca + NanoClik-W9 (8 mg, n=5), W9 (8 mg/kg/day) incorporated in NanoClik nanoparticles was injected into mice fed a low calcium diet; low Ca + NanoClik-W9 (24 mg, n=5), W9 (24 mg/kg/day) incorporated in NanoClik nanoparticles was injected into mice fed a low calcium diet.

prevented the increase in TRAP-positive cells (Figure 5A). The bone histomorphometric analyses revealed that there was a significant increase in bone resorption parameters (osteoclast number and osteoclast surface) in the vehicle-injected low calcium group compared with the vehicle-injected normal calcium group. These increases in bone resorption parameters were significantly reduced in mice injected with W9 24 mg/kg/day incorporated in NanoClik nanoparticles, while the same dose of W9 incorporated in CHP nanogels had no significant effect (Figure 5B and C). These results suggest that the NanoClik nanoparticles are critical for the successful delivery of the peptide drug, W9, to allow it to prevent bone loss by inhibiting excess formation of osteoclasts.

Serum biochemical parameters

In order to clarify whether prevention of bone loss by the NanoClik nanoparticles was due to the reduction of bone resorption activity of osteoclasts, not just to a reduction of osteoclast number, the serum level of CTX, a functional biomarker of bone resorption, was measured. The serum levels of CTX were significantly higher in the vehicle-injected low calcium group compared with the vehicle-injected normal calcium group. Injection of W9 24 mg/kg/day incorporated in NanoClik nanoparticles significantly reduced the serum levels of CTX compared with those in the vehicle-injected low calcium group (Figure 6).

Release profile of W9 from NanoClik nanoparticles in the osteoclastogenesis assay in vitro

To clarify the release profile of W9 from nanogels, we performed a functional assay by counting the number of osteoclasts in a culture with 10% fetal bovine serum, since the W9 peptide has already been shown to act as an inhibitor

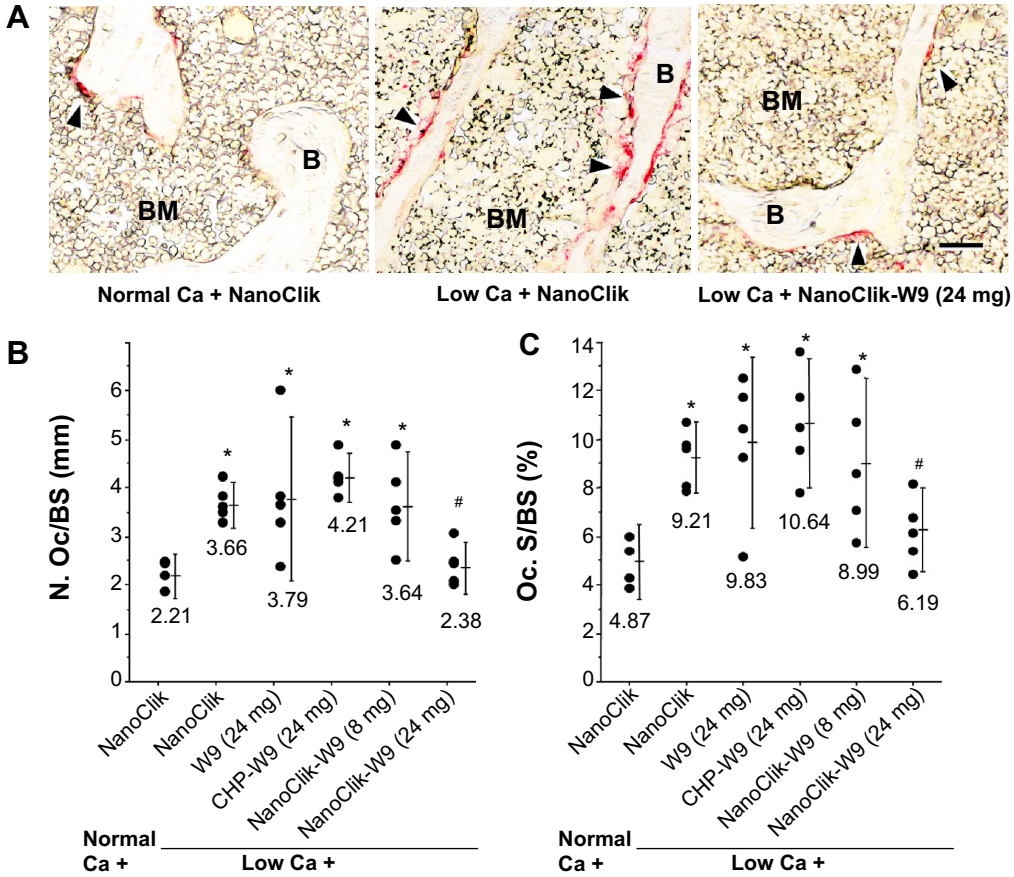

Figure 5 Treatment with W9 24 mg/kg/day complexed in NanoClik nanoparticles prevented the increase in bone resorption parameters induced by a low calcium diet.
Notes: (**A**) Histological observations of the proximal tibiae. TRAP-positive cells are shown in red. TRAP-positive multinucleated cells were designated as osteoclasts. The scale bar represents 50 μm. (**B**) Number of osteoclasts per bone surface and (**C**) osteoclast surface per bone surface. Data are shown as the mean ± standard deviation, with n=5 for each experimental group. *$P<0.05$ versus normal Ca + NanoClik; #$P<0.05$ versus low Ca + NanoClik.
Abbreviations: Ca, calcium; CHP, cholesterol-bearing pullulan; Oc. S/BS, osteoclast surface per bone surface; N. Oc/BS, number of osteoclasts per bone surface; TRAP, tartrate-resistant acid phosphatase; Normal Ca + NanoClik (n=5), vehicle (NanoClik nanoparticle)-injected mice fed a normal calcium diet; low Ca + NanoClik (n=5), vehicle (NanoClik nanoparticle)-injected mice fed a low calcium diet; low Ca + W9 (24 mg, n=5), W9 (24 mg/kg/day) was injected into mice fed a low calcium diet; low Ca + CHP-W9 (24 mg, n=5), W9 (24 mg/kg/day) incorporated in CHP nanogels was injected into mice fed a low calcium diet; low Ca + NanoClik-W9 (8 mg, n=5), W9 (8 mg/kg/day) incorporated in NanoClik nanoparticles was injected into mice fed a low calcium diet; low Ca + NanoClik-W9 (24 mg, n=5), W9 (24 mg/kg/day) incorporated in NanoClik nanoparticles was injected into mice fed a low calcium diet.

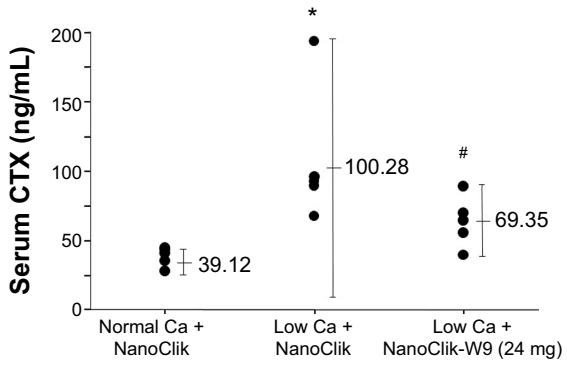

Figure 6 Serum levels of collagen crosslinks.
Notes: Levels of serum CTX, a bone resorption marker, were analyzed by enzyme-linked immunoassay. Data are shown as the mean ± standard deviation, with n=5 for each experimental group. *$P<0.05$ versus normal Ca + NanoClik; #$P<0.05$ versus low Ca + NanoClik.
Abbreviations: Ca, calcium; CTX, C-terminal telopeptide of type I collagen; Normal Ca + NanoClik (n=5), vehicle (NanoClik nanoparticle)-injected mice fed a normal calcium diet; low Ca + NanoClik (n=5), vehicle (NanoClik nanoparticle)-injected mice fed a low calcium diet; low Ca + NanoClik-W9 (24 mg, n=5), W9 (24 mg/kg/day) incorporated in NanoClik nanoparticles was injected into mice fed a low calcium diet.

of osteoclastogenesis.[26] We assumed that the serum-induced free W9 released from nanogels would inhibit osteoclast differentiation, but that the remaining W9 incorporated in nanogels would not. In order to clarify the amount of free W9 released, we established a 4-day osteoclast culture as shown in Figure 7A. We incubated the cells with materials used in the in vivo studies for 3 days (from day 1 to day 4), and stopped the culture on day 4 as described in the Materials and methods section. The osteoclast number, shown as the number of TRAP-positive multinucleated cells, in the CHP-W9-treated cultures was significantly reduced in the presence of 10% fetal bovine serum compared with the cultures exposed to CHP alone ($P<0.05$), but was not significantly reduced in the cultures treated with NanoClik-W9 compared with the cultures exposed to NanoClik nanoparticles, suggesting that the amount of W9 release induced by 10% fetal bovine serum from the NanoClik-W9 was not sufficient to inhibit osteoclastogenesis, while the amount of W9 released from CHP nanogels was sufficient (Figure 7B and C).

To clarify the mechanism underlying the release of W9 from the NanoClik nanoparticles, a higher concentration of fetal bovine serum was used in the same culture system as shown in Figure 7A. As expected, the numbers of TRAP-positive multinucleated cells were significantly decreased in the cultures exposed to NanoClik-W9 compared with the cultures exposed to the NanoClik nanoparticles (Figure 7D), suggesting that the serum proteins might attack the NanoClik-W9 nanogels and push W9 out from the carrier.

In order to reveal further details about the release profile of the NanoClik nanoparticles, we preincubated NanoClik-W9 for 1–5 days with 10% fetal bovine serum-conditioned medium. When we added these preincubated NanoClik-W9 in the osteoclast culture shown in Figure 8A, the number of TRAP-positive multinucleated cells was decreased in a preincubation time-dependent manner (Figure 8B), suggesting that the amount of free W9 released from the NanoClik-W9 nanoparticles was gradually increased in the 10% serum condition with time.

To quantify the amount of W9 released from NanoClik-W9 nanoparticles, the concentration of W9 released from these particles in conditioned medium was determined from the linear regression analysis for the osteoclast numbers versus the corresponding concentrations of W9 (Figure 8C and D). Since 50 μM W9 was applied in NanoClik nanoparticles and around 40 μM W9 was thought to be released from the NanoClik nanoparticles as shown in Figure 8D, we estimated that trapping efficiency of W9 in the NanoClik nanoparticles could be at least 80%.

Discussion

This is the first study to show the feasibility of using our NanoClik nanoparticles as an injectable carrier for peptide drugs. In previous studies, eight daily subcutaneous injections (every 3 hours) of W9 (24 mg/kg/injection) were required to obtain inhibitory effects on low calcium-induced bone resorption when no carrier for the peptide drug was applied.[26,28] In the present study, once-daily subcutaneous injections of W9 24 mg/kg/day incorporated in NanoClik nanoparticles could inhibit the bone loss and osteoclastogenesis induced by a low calcium diet, but single daily injections of W9 incorporated in CHP nanogels could not (Figures 3–5). These results were confirmed by measurement of the serum CTX level, a bone resorption marker that reflects the amount of degradation product of the bone matrix (Figure 6). Therefore, our results indicate that the NanoClik nanoparticles, but not the CHP nanogels alone, allowed W9 to exert inhibitory effects on osteoclastogenesis and bone resorption in vivo by only once-daily subcutaneous injection.

In order to achieve long-term bioactivity of peptide drugs in vivo, it is necessary to inhibit peptide drug aggregation, to allow for sustained release of the peptide drug, and/or to prevent peptide drug degradation.[1] In our study, the CHP nanogels and NanoClik nanoparticles prevented aggregation of W9. However, the inhibitory effects of W9 on bone loss could not be elicited by CHP nanogels containing the drug (Figures 3 and 4). On the other hand, the NanoClik-W9 complex could inhibit bone loss.

Our in vivo findings might be explained by differences in the plasma half-life of the carriers used in this study (Figure 9). We previously showed that the CHP nanogel itself was eliminated from the circulation within 6 hours, while

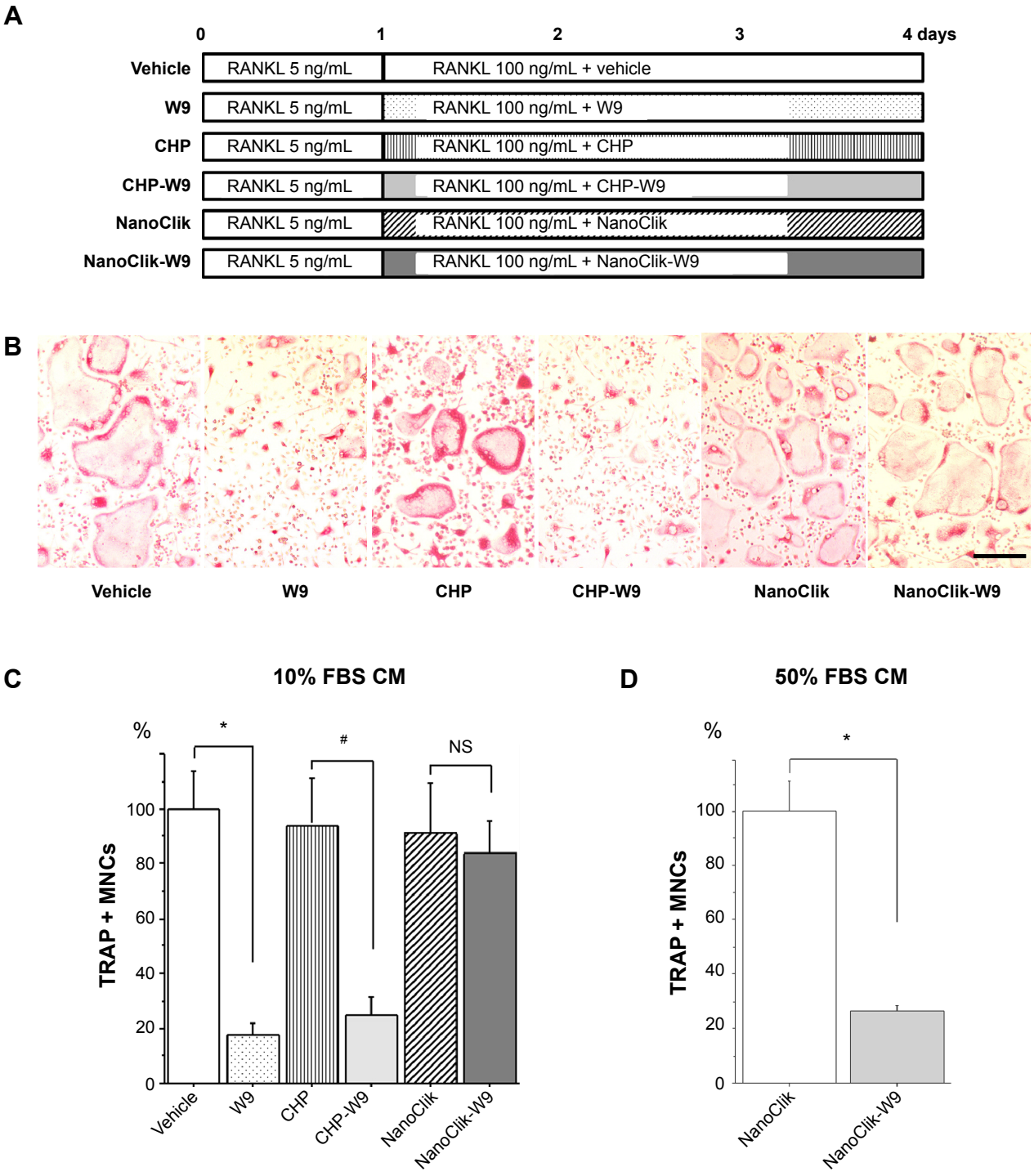

Figure 7 Three-day culture of NanoClik-W9 in 10% FBS was not enough to inhibit osteoclastogenesis, but culture in 50% FBS was sufficient for in vitro inhibition of osteoclastogenesis.

Notes: (**A**) Schematic diagram of the experimental protocol to clarify W9 release mechanism from nanogels in vitro. Murine bone marrow cells were cultured in the presence of 10% FBS, 25 ng/mL M-CSF, and 5 ng/mL RANKL for one day to obtain bone marrow-derived osteoclast precursors. The precursors were then further incubated for 3 days in the presence of 10% FBS, 25 ng/mL M-CSF, and 100 ng/mL RANKL with the materials used in the in vivo study, ie, vehicle (0.05% dimethyl sulfoxide), W9 alone, CHP nanogels, W9 incorporated in CHP nanogels (CHP-W9), NanoClik nanoparticles (NanoClik), and W9 incorporated in NanoClik nanoparticles (NanoClik-W9). (**B**) Representative microscopic images of osteoclast cultures on day 4. TRAP-positive cells are shown in red. The scale bar represents 200 μM. (**C**) TRAP-positive MNCs were counted (n>3). The percentage of TRAP-positive MNCs compared with the vehicle control is shown. *$P<0.05$ versus vehicle; #$P<0.05$ versus CHP conditioned medium. (**D**) Percentage of TRAP-positive MNCs compared with the NanoClik incubated in 50% FBS-conditioned medium using the same protocol as shown in the panel A. The data are shown as the mean ± standard deviation. *$P<0.05$ versus NanoClik.

Abbreviations: CHP, cholesterol-bearing pullulan; CM, conditioned medium; FBS, fetal bovine serum; M-CSF, macrophage colony-stimulating factor; MNCs, multinucleated cells; NS, not significant; RANKL, nuclear factor kappa B ligand; TRAP, tartrate-resistant acid phosphatase.

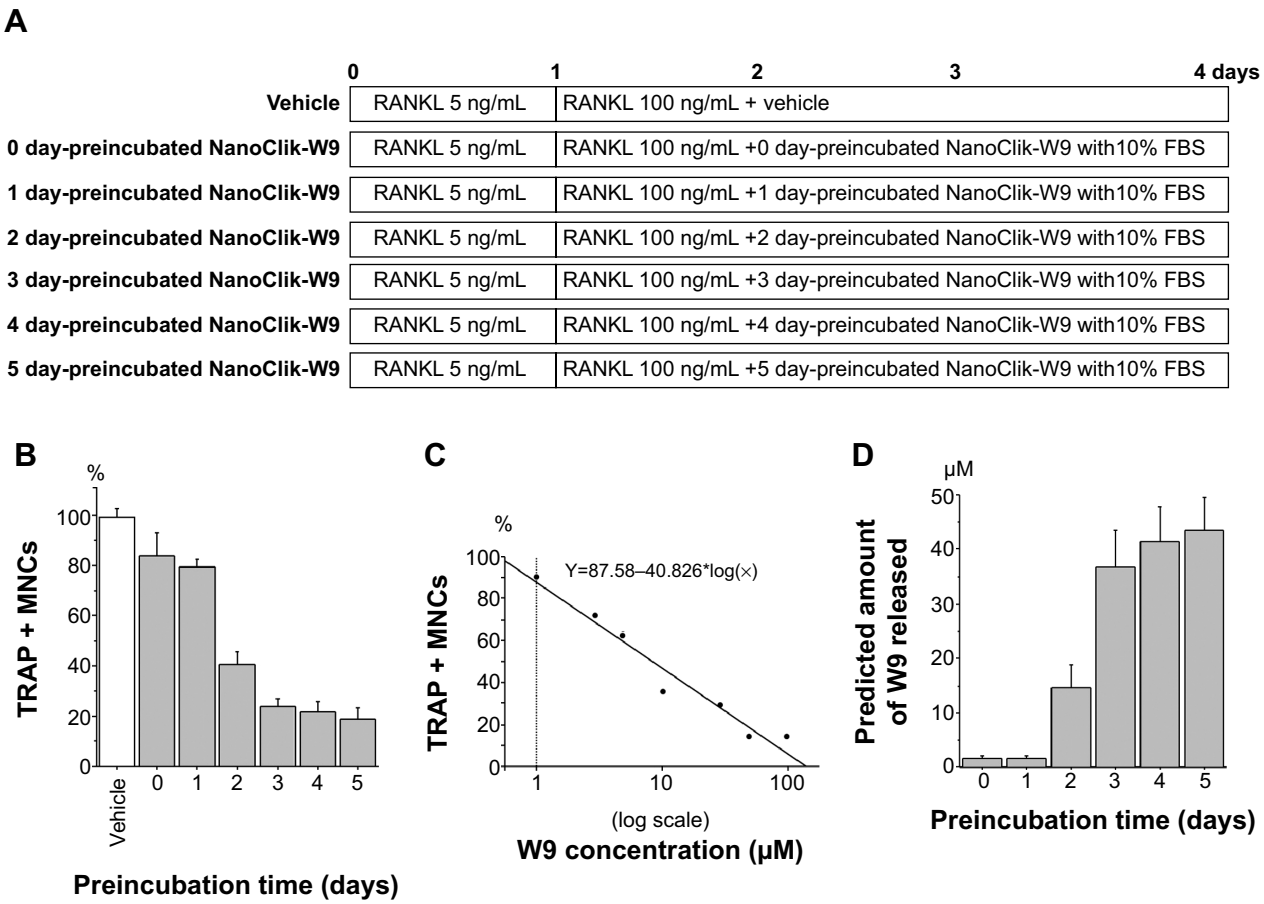

Figure 8 Time-dependent release profile of W9 from NanoClik nanoparticles.
Notes: (**A**) Schematic diagram of the in vitro experimental protocol to show the release profile of W9 in the 10% culture media. NanoClik-W9 was preincubated in 60 μL of 10% FBS alpha-minimal essential medium for 1 to 5 days before adding to the osteoclast culture at day 1. (**B**) TRAP-positive MNCs were counted on day 4. Data are shown as the mean ± standard deviation. The numbers shown in the graph indicate the duration of preincubation of NanoClik-W9 in the 10% FBS conditioned medium. (**C**) Linear regression analysis for the W9 concentrations versus the percentage of TRAP-positive MNCs was performed to predict the released W9 concentration from the inhibition rate of osteoclastogenesis ($R^2 = 0.955$). W9 (1, 3, 5, 10, 30, 50 and 100 μM) was applied to the same culture system as shown in the panel A instead of applying NanoClik-W9. (**D**) Amounts of W9 released from NanoClik nanoparticles in the culture shown in the panel B were predicted using the linear regression analysis shown in the panel C.
Abbreviations: FBS, fetal bovine serum; MNCs, multinucleated cells; RANKL, nuclear factor kappa B ligand; TRAP, tartrate-resistant acid phosphatase.

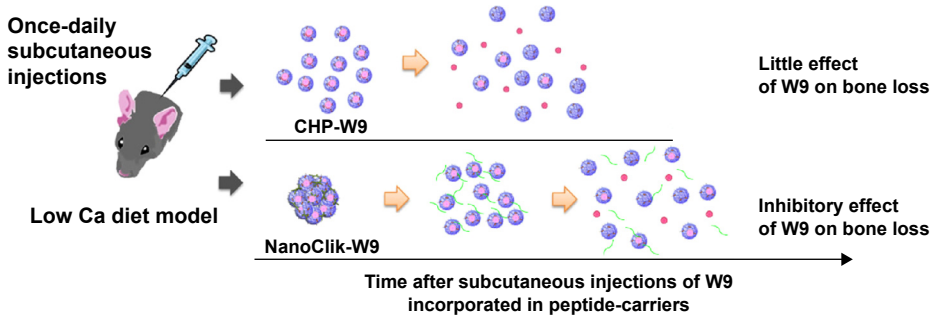

Figure 9 Proposed schema for peptide-drug release from the NanoClik nanoparticles and CHP nanogels.
Notes: The hydrodynamic diameter of W9 incorporated in the NanoClik nanoparticles was larger than that of W9 in the CHP nanogels. After administration of the W9-carrier complex, NanoClik nanoparticles (NanoClik-W9) could sustain the release of W9 better than the CHP nanogels (CHP-W9) due to their decreased degradation. The red circle represents W9, the green line shows PEGSH, and CHP (upper panel) and CHPOA (lower panel) are shown as spherical forms.
Abbreviations: Ca, calcium; CHP, cholesterol-bearing pullulan; CHPOA, acryloyl group-modified cholesterol-bearing pullulan; PEGSH, pentaerythritol tetra (mercaptoethyl) polyoxyethylene.

approximately 40%–50% of the NanoClik nanoparticles remained in the circulation at that point after intravenous injection in mice.[18] NanoClik nanoparticles were previously proven to retain 20%–30% of the nanoparticles derived from the carrier after 24 hours in the circulation.[18] These findings indicate that the NanoClik nanoparticles are more stable than the CHP nanogels in vivo.

Our in vitro studies had provided preliminary information to back up the findings of the in vivo studies, where the results of in vitro studies, especially figure 7C and 7D, demonstrated slower and more controlled release of the therapeutic peptide due to crosslinking compared with the CHP nanogels (Figures 7 and 8). Three days of culture in 10% serum was enough to induce W9 peptide release from the CHP nanogels, but not from the NanoClik nanoparticles, indicating that the NanoClik nanoparticles were essential for the long-term controlled release of the therapeutic peptide (Figure 7B and C). Furthermore, W9 incorporated in NanoClik nanoparticles was proven to inhibit osteoclastogenesis in the 3-day culture with a higher concentration of serum (50%), but not in that with a lower concentration of serum (10%), providing insight into the mechanism underlying the release of the peptide from the NanoClik nanoparticles, where there is an exchange with serum proteins to release the incorporated peptide (Figure 7C and D). The results showing the preincubation time-dependent release profile of W9 from the NanoClik nanoparticles in the 10% fetal bovine serum-conditioned medium confirmed the slower and more controlled release from these nanoparticles compared with the CHP nanogels (Figure 8).

The inhibitory effects of W9 on bone resorption in this study could be due to the protein-repellant properties of the NanoClik nanoparticles. Since the hydrophilic characteristics of PEG are known to prevent protein adsorption,[24,25] the PEG-crosslinked carrier itself is considered to be more protective against the surrounding proteins, including protein degradation enzymes, compared with CHP nanogels, which could lead to a reduction in degradation of the CHP carrier. On the other hand, W9 is thought to be released by an exchange mechanism involving surrounding proteins like serum albumin. Therefore, the protein-repellant properties of the PEGylated carrier might have also prevented the release of W9, further promoting the long-term inhibitory effects of W9 on bone loss in vivo.

In conclusion, NanoClik nanoparticles showed potential as a novel sustained-release carrier for peptide drugs. Our findings clarify the feasibility of using NanoClik nanoparticles as an injectable carrier for peptide drugs in vivo.

Acknowledgment

This work was supported by the grants from Japan Society for the Promotion of Science Grants-in-Aid for Scientific Research (19390472, 23659867 and 25293377 to KAoki and 22-00432 and 24390413 to KO).

Disclosure

The authors report no conflicts of interest in this work.

References

1. Aoki K, Alles N, Soysa N, Ohya K. Peptide-based delivery to bone. *Adv Drug Deliv Rev.* 2012;64(12):1220–1238.
2. Kieber-Emmons T, Murali R, Greene MI. Therapeutic peptides and peptidomimetics. *Curr Opin Biotechnol.* 1997;8(4):435–441.
3. Lowman HB. Bacteriophage display and discovery of peptide leads for drug development. *Annu Rev Biophys Biomol Struct.* 1997;26:401–424.
4. Malavolta L, Pinto MR, Cuvero JH, Nakaie CR. Interpretation of the dissolution of insoluble peptide sequences based on the acid-base properties of the solvent. *Protein Sci.* 2006;15(6):1476–1488.
5. Shive MS, Anderson JM. Biodegradation and biocompatibility of PLA and PLGA microspheres. *Adv Drug Deliv Rev.* 1997;28(1):5–24.
6. Hutchinson FG, Furr BJ. Biodegradable polymers for controlled release of peptides and proteins. *Horiz Biochem Biophys.* 1989;9:111–129.
7. Lee K, Yuk S. Polymeric protein delivery systems. *Prog Polym Sci.* 2007;32(7):669–697.
8. Mao S, Sun W, Kissel T. Chitosan-based formulations for delivery of DNA and siRNA. *Adv Drug Deliv Rev.* 2010;62(1):12–27.
9. Kataoka K, Harada A, Nagasaki Y. Block copolymer micelles for drug delivery: design, characterization and biological significance. *Adv Drug Deliv Rev*. 2001;47(1):113–131.
10. Niu X, Feng Q, Wang M, Guo X, Zheng Q. Porous nano-HA/collagen/PLLA scaffold containing chitosan microspheres for controlled delivery of synthetic peptide derived from BMP-2. *J Control Release.* 2009;134(2):111–117.
11. Akiyoshi K, Deguchi S, Moriguchi N, Yamaguchi S, Sunamoto J. Self-aggregates of hydrophobized polysaccharides in water-formation and characeristics of nanoparticles. *Macromolecules.* 1993;26(12):3062–3068.
12. Akiyoshi K, Kobayashi S, Shichibe S, et al. Self-assembled hydrogel nanoparticle of cholesterol-bearing pullulan as a carrier of protein drugs: complexation and stabilization of insulin. *J Control Release.* 1998;54(3):313–320.
13. Akiyoshi K, Deguchi S, Sunamoto J, Nishikawa T, Sunamoto J. Microscopic structure and thermoresponsiveness of a hydrogel nanoparticle by self-assembly of a hydrophobized polysaccharide. *Macromolecules.* 1997;30(4):857–861.
14. Morimoto N, Endo T, Iwasaki Y, Akiyoshi K. Design of hybrid hydrogels with self-assembled nanogels as cross-linkers: interaction with proteins and chaperone-like activity. *Biomacromolecules.* 2005;6(4):1829–1834.
15. Uenaka A, Wada H, Isobe M, et al. T cell immunomonitoring and tumor responses in patients immunized with a complex of cholesterol-bearing hydrophobized pullulan (CHP) and NY-ESO-1 protein. *Cancer Immun.* 2007;7:9.
16. Kitano S, Kageyama S, Nagata Y, et al. HER2-specific T-cell immune responses in patients vaccinated with truncated HER2 protein complexed with nanogels of cholesteryl pullulan. *Clin Cancer Res.* 2006;12(24):7397–7405.
17. Shimizu T, Kishida T, Hasegawa U, et al. Nanogel DDS enables sustained release of IL-12 for tumor immunotherapy. *Biochem Biophys Res Commun.* 2008;367(2):330–335.
18. Shimoda A, Sawada S, Kano A, et al. Dual crosslinked hydrogel nanoparticles by nanogel bottom-up method for sustained-release delivery. *Colloids Surf B Biointerfaces.* 2012;99:38–44.

19. Cheng J, Teply BA, Sherifi I, et al. Formulation of functionalized PLGA-PEG nanoparticles for in vivo targeted drug delivery. *Biomaterials.* 2007; 28(5):869–876.
20. Li Y, Pei Y, Zhang X, et al. PEGylated PLGA nanoparticles as protein carriers: synthesis, preparation and biodistribution in rats. *J Control Release.* 2001;71(2):203–211.
21. Essa S, Rabanel JM, Hildgen P. Effect of polyethylene glycol (PEG) chain organization on the physicochemical properties of poly(D, L-lactide) (PLA) based nanoparticles. *Eur J Pharm Biopharm.* 2010;75(2):96–106.
22. Zalipsky S, Harris J. Introduction to chemistry and biological applications of poly(ethylene glycol), 1997. Available from: http://pubs.acs.org/doi/pdf/10.1021/bk-1997-0680.ch001. Accessed December 28, 2014.
23. Hashimoto Y, Mukai SA, Sawada S, Sasaki Y, Akiyoshi K. Nanogel tectonic porous gel loading biologics, nanocarriers, and cells for advanced scaffold. *Biomaterials.* 2015;37:107–115.
24. Wang R, Kreuzer H, Grunze M. Molecular conformation and solvation of oligo(ethylene glycol)-terminated self-assembled monolayers and their resistance to protein adsorption. *J Phys Chem B*. 1997;101(47): 9767–9773.
25. Elbert DL, Hubbell JA. Self-assembly and steric stabilization at heterogeneous, biological surfaces using adsorbing block copolymers. *Chem Biol.* 1998;5(3):177–183.
26. Aoki K, Saito H, Itzstein C, et al. A TNF receptor loop peptide mimic blocks RANK ligand-induced signaling, bone resorption, and bone loss. *J Clin Invest.* 2006;116(6):1525–1534.
27. Aoki K, Maeda M, Nakae T, Okada Y, Ohya K, Chiba K. A disulfide bond replacement strategy enables the efficient design of artificial therapeutic peptides. *Tetrahedron.* 2014;70(42):7774–7779.
28. Saito H, Kojima T, Takahashi M, et al. A tumor necrosis factor receptor loop peptide mimic inhibits bone destruction to the same extent as anti-tumor necrosis factor monoclonal antibody in murine collagen-induced arthritis. *Arthritis Rheum.* 2007;56(4):1164–1174.
29. Alles N, Soysa NS, Hussain MD, et al. Polysaccharide nanogel delivery of a TNF-α and RANKL antagonist peptide allows systemic prevention of bone loss. *Eur J Pharm Sci.* 2009;37(2):83–88.
30. Sato K, Suematsu A, Nakashima T, et al. Regulation of osteoclast differentiation and function by the CaMK-CREB pathway. *Nat Med.* 2006; 12(12):1410–1416.
31. Kojima T, Aoki K, Nonaka K, et al. Subcutaneous injections of a TNF-alpha antagonistic peptide inhibit both inflammation and bone resorption in collagen-induced murine arthritis. *J Med Dent Sci.* 2005; 52(1):91–99.
32. Suzuki Y, Aoki K, Saito H, et al. A tumor necrosis factor-alpha antagonist inhibits inflammatory bone resorption induced by Porphyromonas gingivalis infection in mice. *J Periodontal Res.* 2006;41(2):81–91.
33. Seto H, Aoki K, Kasugai S, Ohya K. Trabecular bone turnover, bone marrow cell development, and gene expression of bone matrix proteins after low calcium feeding in rats. *Bone.* 1999;25(6):687–695.
34. Beamer WG, Shultz KL, Donahue LR, et al. Quantitative trait loci for femoral and lumbar vertebral bone mineral density in C57BL/6J and C3H/HeJ inbred strains of mice. *J Bone Miner Res.* 2001;16(7): 1195–1206.
35. Nakachi H, Aoki K, Tomomatsu N, et al. A structural modulator of tumor necrosis factor type 1 receptor promotes bone formation under lipopolysaccharide-induced inflammation in a murine tooth extraction model. *Eur J Pharmacol.* 2012;679(1–3):132–138.
36. Alles N, Soysa NS, Hayashi J, et al. Suppression of NF-kappaB increases bone formation and ameliorates osteopenia in ovariectomized mice. *Endocrinology.* 2010;151(10):4626–4634.
37. Nagahama K, Aoki K, Nonaka K, et al. The deficiency of immunoregulatory receptor PD-1 causes mild osteopetrosis. *Bone.* 2004; 35(5):1059–1068.
38. Parfitt AM, Drezner MK, Glorieux FH, et al. Bone histomorphometry: standardization of nomenclature, symbols, and units. Report of the ASBMR Histomorphometry Nomenclature Committee. *J Bone Miner Res.* 1987;2(6):595–610.
39. Dempster DW, Compston JE, Drezner MK, et al. Standardized nomenclature, symbols, and units for bone histomorphometry: a 2012 update of the report of the ASBMR Histomorphometry Nomenclature Committee. *J Bone Miner Res.* 2013;28(1):2–17.
40. Lacey DL, Timms E, Tan HL, et al. Osteoprotegerin ligand is a cytokine that regulates osteoclast differentiation and activation. *Cell.* 1998; 93(2):165–176.
41. Yasuda H, Shima N, Nakagawa N, et al. Identity of osteoclastogenesis inhibitory factor (OCIF) and osteoprotegerin (OPG): a mechanism by which OPG/OCIF inhibits osteoclastogenesis in vitro. *Endocrinology.* 1998;139(3):1329–1337.

Supplementary materials

Concerning our in vivo model

Our low calcium diet model was established in 1989, and has been used extensively since then.[1–8] These numerous studies have shown comparable serum calcium levels during the experimental period, although the ionized calcium levels were lower in the low calcium diet group compared with the normal calcium diet group. Furthermore, treatment with a bone resorption inhibitor (clodronate, a bisphosphonate) did not change the serum calcium levels.[7]

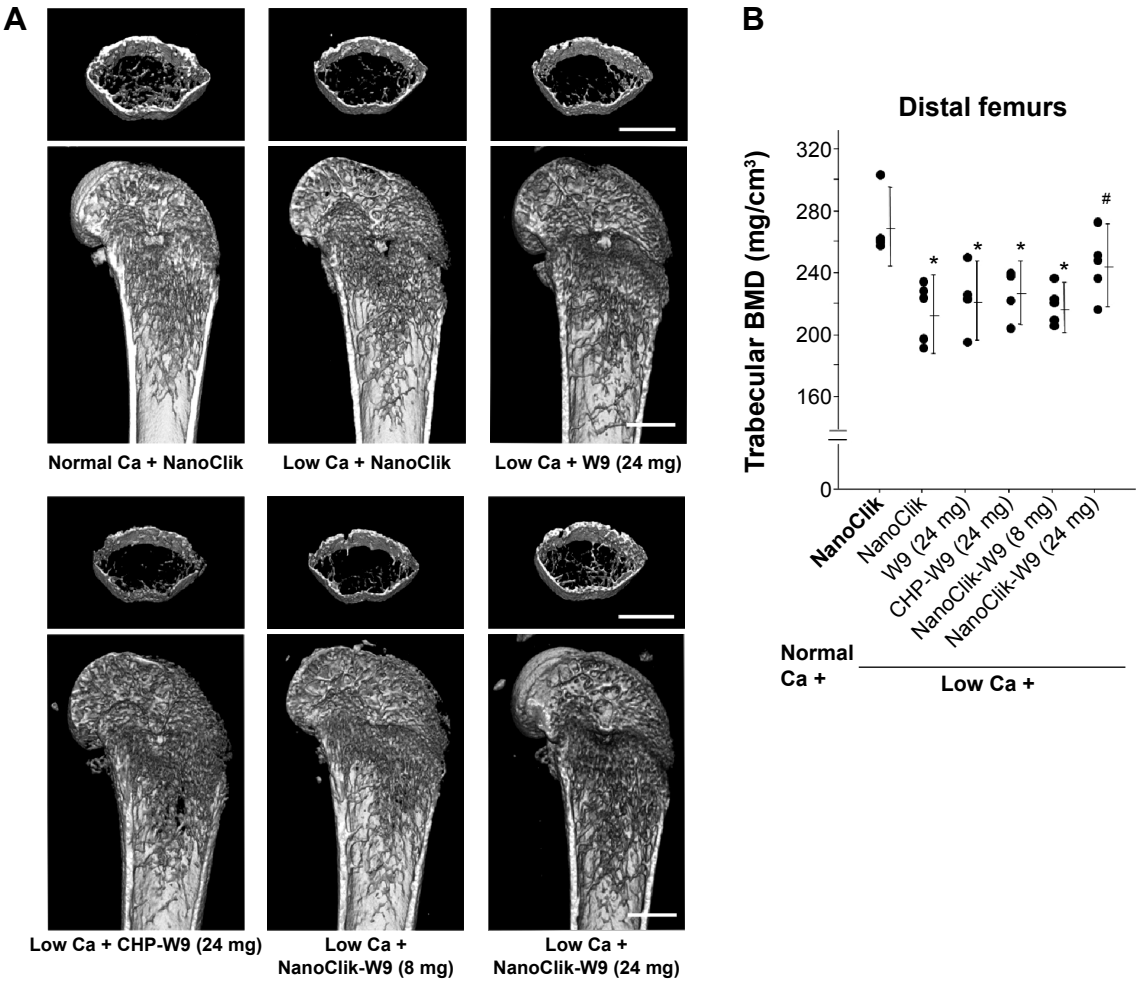

Figure S1 Radiological assessment of distal femurs.

Notes: (**A**) Three-dimensional reconstruction images of distal femurs examined by microfocal computed tomography. Top, an axial view of transverse bone segments at the metaphysis; bottom, the longitudinal view. The bar represents 1 mm. (**B**) Results of a quantitative analysis of femoral trabecular BMD at the distal metaphysis measured by peripheral quantitative computed tomography. Data are shown as the mean ± standard deviation, with n=5 for each experimental group. $^{*}P<0.05$ versus normal Ca + NanoClik; $^{\#}P<0.05$ versus low Ca + NanoClik.

Abbreviations: BMD, bone mineral density; Ca, calcium; CHP, cholesterol-bearing pullulan; Normal Ca + NanoClik (n=5), vehicle (NanoClik nanoparticle)-injected mice fed a normal calcium diet; low Ca + NanoClik (n=5), vehicle (NanoClik nanoparticle)-injected mice fed a low calcium diet; low Ca + W9 (24 mg, n=5), W9 (24 mg/kg/day) was injected into mice fed a low calcium diet; low Ca + CHP-W9 (24 mg, n=5), W9 (24 mg/kg/day) incorporated in CHP nanogels was injected into mice fed a low calcium diet; low Ca + NanoClik-W9 (8 mg, n=5), W9 (8 mg/kg/day) incorporated in NanoClik nanoparticles was injected into mice fed a low calcium diet; low Ca + NanoClik-W9 (24 mg, n=5), W9 (24 mg/kg/day) incorporated in NanoClik nanoparticles was injected into mice fed a low calcium diet.

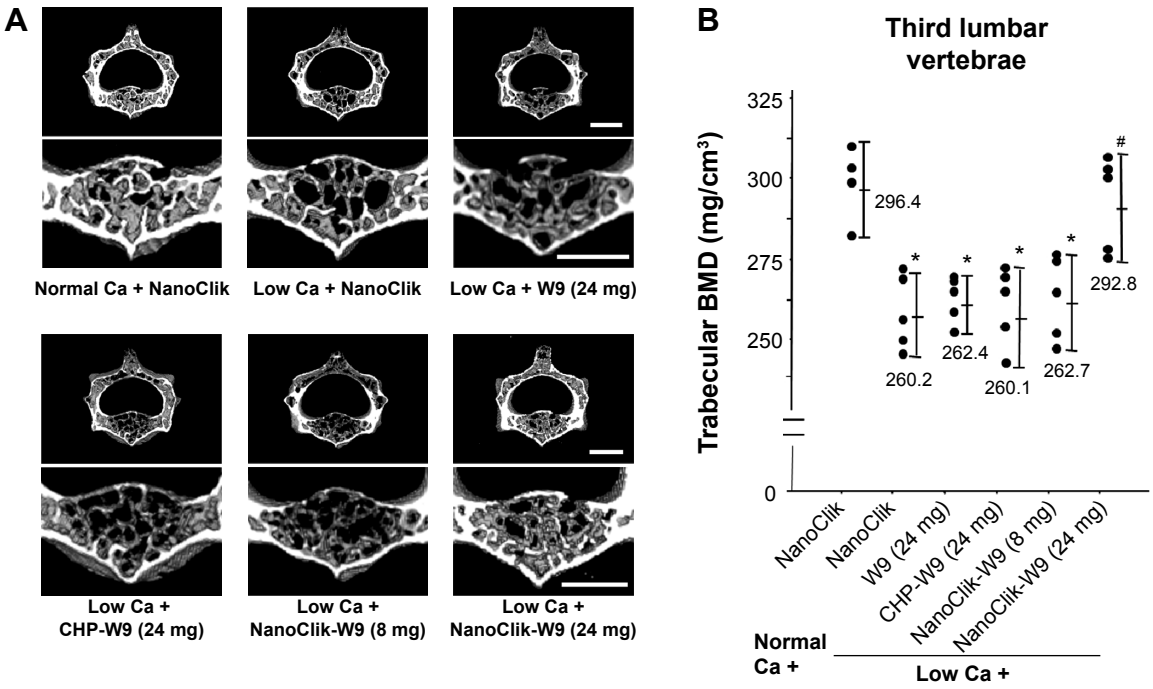

Figure S2 Radiological assessments of the third lumbar vertebrae.

Notes: (**A**) Three-dimensional reconstruction images (upper panel) and trabecular-rich region (lower panel) of the third lumbar vertebrae were examined by microfocal computed tomography. The bar represents 1 mm. (**B**) Results of a quantitative analysis of trabecular BMD at the vertebral body measured by peripheral quantitative computed tomography. The data are shown as the mean ± standard deviation with n=5 for each experimental group. *$P<0.05$ versus normal Ca + NanoClik; #$P<0.05$ versus low Ca + NanoClik.

Abbreviations: BMD, bone mineral density; Ca, calcium; CHP, cholesterol-bearing pullulan; Normal Ca + NanoClik (n=5), vehicle (NanoClik nanoparticle)-injected mice fed a normal calcium diet; low Ca + NanoClik (n=5), vehicle (NanoClik nanoparticle)-injected mice fed a low calcium diet; low Ca + W9 (24 mg, n=5), W9 (24 mg/kg/day) was injected into mice fed a low calcium diet; low Ca + CHP-W9 (24 mg, n=5), W9 (24 mg/kg/day) incorporated in CHP nanogels was injected into mice fed a low calcium diet; low Ca + NanoClik-W9 (8 mg, n=5), W9 (8 mg/kg/day) incorporated in NanoClik nanoparticles was injected into mice fed a low calcium diet; low Ca + NanoClik-W9 (24 mg, n=5), W9 (24 mg/kg/day) incorporated in NanoClik nanoparticles was injected into mice fed a low calcium diet.

References

1. Amano H et al, A histomorphometric analysis of the alveolar bone resorption process in calcium-deficient rats. *J Oral Biosci*. 1989 (31) No.4
2. Aoki K et al, Differential response in the cortical and the cancellous regions of tibia to a low calcium feeding in rats: A histomorphometric study *J Oral Biosci*. 1992 (34) No.5
3. Seto H, Aoki K, Kasugai S, Ohya K. Trabecular bone turnover, bone marrow cell development, and gene expression of bone matrix proteins after low calcium feeding in rats. *Bone*. 1999;25(6):687–695.
4. Aoki K, Saito H, Itzstein C, et al. A TNF receptor loop peptide mimic blocks RANK ligand-induced signaling, bone resorption, and bone loss. *J Clin Invest*. 2006;116(6):1525–1534.
5. Alles N, Soysa NS, Hussain MD, et al. Polysaccharide nanogel delivery of a TNF-α and RANKL antagonist peptide allows systemic prevention of bone loss. *Eur J Pharm Sci*. 2009;37(2):83–88.
6. Aoki K, Maeda M, Nakae T, Okada Y, Ohya K, Chiba K. A disulfide bond replacement strategy enables the efficient design of artificial therapeutic peptides. *Tetrahedron*. 2014;70(42):7774–7779.
7. Horie D, Takahashi M, Aoki K, Ohya K. Clodronate stimulates bone formation as well as inhibits bone resorption and increases bone mineral density in rats fed a low-calcium diet. *J Med Dent Sci*. 2003;50(1):121–132.
8. Sato K, Suematsu A, Nakashima T, et al. Regulation of osteoclast differentiation and function by the CaMK-CREB pathway. *Nat Med*. 2006;12(12):1410–1416.